



Wind tunnel measurements of concentration fluctuations in an urban street canyon

Michel Pavageau^{a,*}, Michael Schatzmann^b

^a*Ecole des Mines de Nantes, Departement Systèmes Energétiques et Environnement, 4, Rue Alfred Kastler, BP 20722, 44307 Nantes Cedex 03, France*

^b*Meteorologisches Institut, Hamburg Universität, Bundesstraße 55, 20146 Hamburg, Germany*

Abstract

A wind tunnel study was performed to examine some turbulent characteristics and statistical properties of the concentration field developing from the steady release of a tracer gas at street level in a canyon amidst urban roughness. The experiment was conducted with the approaching wind direction perpendicular to the street axis and, with a street width to building height aspect ratio equal to one. Concentration time series were recorded at 70 points within the test street cross-section and above. Mean concentrations, variances and related turbulent quantities, as well as other statistical quantities including quantiles were computed. Concentration spectra and autocorrelation functions were also examined. The emphasis is put here on the results concerning mean concentrations and the variance of concentration fluctuations. The main objective of this paper is to put forward potential benefits of the experimental approach taken in this study. Through a simple and already widely studied configuration it is aimed to show how, for modelling purposes, this approach can help improving our understanding of the mechanisms of dispersion of pollution from car exhausts in built-up areas and, with further measurements, how it could assist in drawing specifications for siting monitoring networks. © 1999 Elsevier Science Ltd. All rights reserved.

Keywords: Turbulent concentration field; Wind tunnel modelling; Vehicular emissions; Built-up areas; Pollution dispersion

1. Introduction

In response to an increasing concern for environmental issues and in particular for sustainable air quality standards in cities, a plethora of urban pollution dispersion models came into being during the last decade. Routinely used by regulatory bodies, architects or town planners, most currently available operational models are usually limited to providing information about hourly mean concentrations. Their reliability in predicting probabilistic statements about deviations from the predicted mean concentrations is often questionable (Hanna, 1993). Yet, these quantities can sometimes be of interest as well.

Clearly, the development of simple models able to provide statistical information on air pollutant concen-

tration distributions in urban areas has been hampered by a lack of knowledge regarding the turbulent, and hence statistical, aspect of pollution dispersion mechanisms in the urban canopy. In physical modelling attention so far has actually been focused mainly on mean concentration levels and their spatial distribution for a wide range of scenarios from combinations of various source types, building arrangements, and approaching flow configurations. The probabilistic aspect of the problem has been rather neglected, although the nature of air flows in built-up areas, by itself, should have justified that the turbulent characteristics of concentration fluctuations be studied more thoroughly.

It has been shown that extreme events like peak values, probability that concentrations will exceed a certain threshold, average rates of excursion beyond this threshold could be derived from predictions, as a function of time and space, of mean concentrations and variances together with probability distribution functions. Relevant

* Corresponding author.

discussions can be found in Chatwin and Sullivan (1993), Kristensen (1994) and Wilson (1995). Although these are mostly related to plume dispersion in the unobstructed atmosphere, general concepts presented therein are, nevertheless, of general scope. The relevant approaches need to be extended to the case of built-up areas.

One possible way of improving our knowledge in that field is to experimentally study the behaviour of concentration fluctuations, and the interaction between turbulence scales in the urban canopy and the lower part of the atmospheric boundary layer. This can be achieved from simultaneous measurements of turbulent velocities and concentrations and from the examination of the balance of the terms forming the relevant variance and flux transport equations. Such investigations, besides, will serve the development in progress of higher-order models designed to overcome the inherent limitations of currently used urban pollution dispersion models which are often based on the gradient-transfer approach.

In addition, as was pointed out by Olesen (1995), the validity of dispersion model evaluation usual procedures is doubtful. These rest on the comparison between experimental and numerical results. The fact is that these comparisons are often made at a few points only, because, in field or wind tunnel experiments, measurements are taken at a too often limited number of points. In particular, in most wind tunnel experiments, concentrations are usually measured only on building walls or at street level. Samplings should be extended to points within the street cavities as numerical models are expected to provide concentrations at all points in space.

Therefore, a wind tunnel investigation has been initiated of the statistical behaviour and properties of the pollutant field in a street canyon amidst urban roughness. In this study, the analysis was restricted to the case of a continuous and steady release of pollution at ground level with the external wind perpendicular to the street axis. Time series of fluctuating concentrations were recorded at an unusually large number of points covering the whole cross-section of the test street. Data were analysed with the view to providing modellers with a comprehensive data set including mean values, variances and associated statistical quantities. Energy spectra, relevant autocorrelation functions and density probability functions were examined as well.

The physical modelling techniques used in the present study are only briefly outlined in this paper. More details can be found in Donat (1989), Meroney et al. (1996) and references therein. The experimental set-up is described with a particular emphasis on the measurement procedures. The objectives of this paper are mainly to present the approach taken for this analysis, and to show potential benefits from it. This is illustrated through a presentation of the experimental results for mainly the mean concentration and variance fields.

2. Experimental set-up

2.1. Simulation of the atmospheric boundary layer

The atmospheric wind tunnel of the University of Hamburg is of open circuit type. The effective working section is 1 m high, 1.5 m wide and 4 m long following a 7.5 m long development section just downstream of the boundary layer simulation system. The wind tunnel is used primarily to simulate neutral flows as was the case in this experiment. Its adjustable ceiling allows minimisation of the longitudinal pressure gradient over the working section (typically, -0.1 Pa m^{-1} for 3 m s^{-1} free stream velocity).

The atmospheric boundary layer is generated by means of four 750 mm high Irwin-type vortex generators laterally spaced and symmetrical to the tunnel centreline at intervals of half the height of the spires (Irwin, 1979, 1981). The simulated boundary layer is about 450 mm thick. The vertical velocity distribution in the region where the boundary layer is fully developed, can be described by a power law,

$$\frac{U(z)}{U_{\text{ref}}} = \left(\frac{z - d_0}{z_{\text{ref}} - d_0} \right)^\alpha, \quad (1)$$

where d_0 is the displacement height, $U(z)$ the mean velocity at elevation z , and U_{ref} is the mean velocity at the reference height z_{ref} .

In the open wind tunnel, i.e. in the absence of any model, with 20 mm high Lego™ elements placed on the floor in a regular array following a low-density staggered pattern (see Meroney et al., 1996), and for various external velocities taken in the free region of the flow at a reference height z_{ref} of 650 mm above the floor, the vertical wind profile exponent α and the displacement height d_0 were estimated to 0.28 and 2 mm, respectively. The roughness length z_0 , determined from a logarithmic profile up to 120 mm above the floor was about 1.7 mm. The velocity ratio U^*/U_{ref} where U^* is the friction velocity, was found of the order of 0.074¹.

This arrangement corresponds to a simulation of the atmospheric surface layer at a scale of about 1 : 500. Donat (1989) performed additional experiments including spectral analysis and measurements of turbulence intensity for all three components of the velocity. He showed that there was a high degree of coincidence between the characteristics of the boundary layer created in this manner and those found in nature.

¹ It is here essential to precise that U^* was not inferred from measurements of turbulent-flux profiles but from a curve fitting of vertical velocity profiles in the lower 12 cm of the boundary layer.

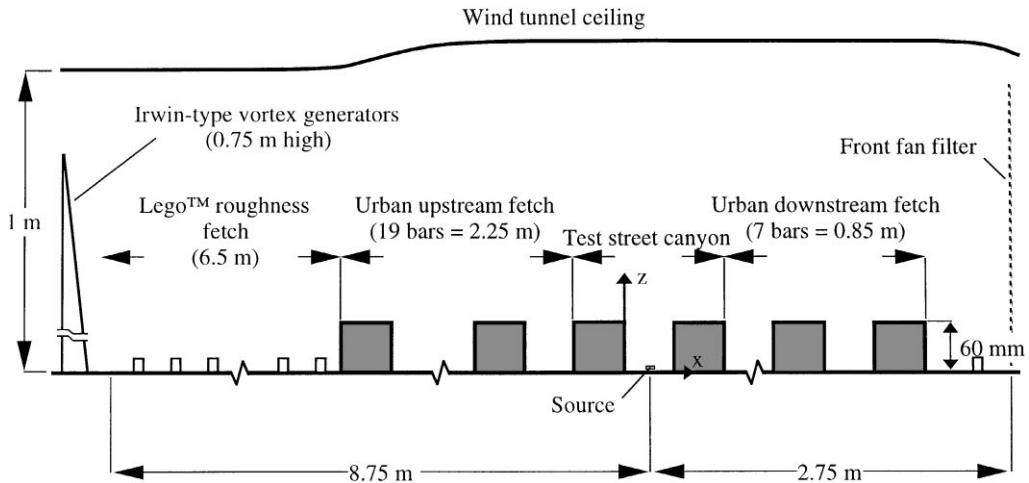


Fig. 1. Side view of the two-dimensional urban model (flow direction from left to right).

2.2. Urban modelling

Building models were made of aluminium U -profiles to give good size accuracy. They were of uniform size $1.4 \times 0.06 \times 0.06$ m. The blocks were laid on the wind tunnel floor perpendicularly to the mean flow direction, almost completely spanning the width of the wind tunnel. They were equally spaced 0.06 m from each other so as to form a regular set of parallel street canyons with a constant aspect ratio of street width to building height equal to one (Fig. 1). The test street canyon was located 8.75 m downstream of the vortex generators. A long urban fetch consisting of 19 bars and a shorter fetch of 7 bars were provided upwind and downwind, respectively. The reasons for such an arrangement, instead of an isolated street canyon amidst open country, have been discussed by Meroney et al. (1996). This configuration corresponds to a two-dimensional simulation at a scale of 1 : 500 of an idealised large city with 30 m high tall buildings. Upstream and downstream of the urban model, the floor of the wind tunnel was covered with 20 mm high Lego™ elements placed in a regular array following a staggered pattern as identical to that used in the open country case.

From several vertical wind profiles taken above the test canyon and the buildings immediately upstream and downstream of it, averaged values of α and d_0 were estimated to 0.21 and 60 mm, respectively, for this arrangement. Derived from the relevant logarithmic profiles, the averaged roughness length z_0 was estimated to about 0.5 mm, and the averaged velocity ratio U^*/U_{ref} was found to be of the order of 0.05, with U_{ref} taken at a reference height of 440 mm above the model roof level. Thus, introducing the urban model in the wind tunnel has two major effects on the approaching flow: (i) the boundary layer is displaced upwards of a height equal to

the building height, and (ii) the flow partly loses memory of the roughness conditions prevailing over the Lego fetch, and, in the present case accommodates to smoother roughness conditions despite the size of the blocks and that of the gaps separating them. Following the picture suggested by the nomenclature of Oke (1988), the approaching flow looks as if it was gently skimming the urban model. The roughness Reynolds number U^*z_0/ν was larger than 2.5 as recommended by Snyder (1972)², and the Reynolds number based on the building height and the mean velocity at the roof level, was above the critical value of 3400 ensuring that the flow pattern in the street canyon was independent of viscous effects (Hoydysh et al., 1974)³. This was checked for through several tests performed at various free stream velocities.

2.3. Emission modelling

A 0.9 m long line-source consisting of a row of 302 point-sources was centred in the test canyon at the street level. The source was covered with a thin metal strip canopy so that any initial vertical gas momentum was deflected laterally. The design in itself of this line source already formed the subject of a previous paper (Meroney et al., 1996) within which earlier tests proving the good lateral evenness of the tracer gas discharge from the source have been reported. We shall not elaborate here further on this point.

² Plate (1982) suggested 5 instead of 2.5.

³ Alternative values have actually been suggested by other authors (Golden, 1961; Snyder, 1992). For urban roughness the suggestion by Hoydysh et al. (1974) is appropriate. For a discussion on that point refer to Meroney et al. (1996).

The tracer gas used in this experiment was a mixture of ethane and air with approximate flow rates of 4 and 150 l h⁻¹, respectively. The concentration of hydrocarbons in the compressed-air supply used in the tracer gas mixture was of the order of 0.5 ppm, i.e. several orders of magnitude below the mean concentration levels encountered in the street cavity during experiments (see Section 3.1). Therefore, the contamination of the air supply with hydrocarbons was not accounted for in the analysis.

The discharge flow from the exhaust holes of the source is laminar. The turbulence intensity of concentration fluctuations⁴ measured at the source outlets in the absence of wind was about 4%, i.e., one order of magnitude less than the average turbulence intensity of concentration fluctuations over the street cross-section during experiments (see Section 3.2). Therefore, the turbulence generated solely by the tracer gas discharge in the test street marginally contributes to the overall level of turbulence in the test canyon which is primarily determined by the turbulent characteristics of the flow inside the street.

2.4. Measurement techniques

The rotation speed of the wind tunnel fan was kept constant during the experiment to achieve a steady free stream velocity of about 3 m s⁻¹. This was monitored with a Prandtl tube and a single hot-wire. Both were positioned at the wind tunnel centreline, 50 cm above the floor, a few centimetres upstream of the leading edge of the upstream urban fetch. During measurements, the signals from the Prandtl tube and the hot-wire were digitally recorded for 60 s on a personal computer. The relevant time-averaged velocities were computed on-line. The mean of these two values was taken later in the non-dimensionalisation process of concentrations. Note that the indications from the Prandtl tube and the hot-wire never departed more than 2% from their mean.

The detection of tracer concentrations was achieved with a fast flame ionisation detector (FID) model HFR400 from Cambustion Ltd. A straight 200 mm long sampling capillary tube 0.254 mm inner diameter was mounted on the fast FID head. The sampling tube was reinforced by slipping its upper half into a 10 cm long rigid tube of outer diameter 1.5 mm to prevent undesired oscillations of the probe tip around its position and, thus, to avoid the introduction of fictitious concentration fluctuations through sampling at a spatially variable

measurement point. The combustion chamber was covered with a streamlined protective sheath to minimise cooling from the oncoming flow, and to keep the temperature of the chamber as constant as possible during the whole duration of the experiment. The pressure difference across the sampling tube was set to 250 mmHg to obtain a frequency response of the sensing system of the order of 170 Hz estimated through dynamical calibration of the device. It was ensured that, for all sampling locations, the combustion chamber was positioned far enough from the test site not to affect the flow pattern in the street cavity.

An estimate of the maximum frequency likely to be encountered in the street canyon flow is given by

$$f_{\max} = \frac{U_{\text{adv}}}{\eta_{\min}}, \quad (2)$$

where η_{\min} is the characteristic size of the smallest eddies present in the street canyon, and U_{adv} is the maximum velocity at which eddies are convected. We shall assume that the Kolmogorov microscale of concentration η_c is about 0.1 mm and that molecular diffusion operates at scales $10\eta_c$ (and smaller). Taking $\eta_{\min} = 10\eta_c$ and assuming that the maximum advective velocity $U_{\text{adv}} \approx 0.66 U_{\text{roof}}$ (De Paul and Sheih, 1984; Nakamura and Oke, 1988), and $U_{\text{roof}} \approx 0.3U(\delta)$ where δ is the boundary layer height, then this yields $f_{\max} \approx 600$ Hz for a free stream velocity of 3 m s⁻¹. This indicates that the fast FID is not able to resolve the entire range of turbulent scales involved in the turbulent dispersion process in this case. However, dispersion is dominated by the action of the largest scales. Moreover, the turbulent scales associated with dissipation processes contribute little to the value of the statistical moments of interest in this analysis. Therefore, it is more essential that the system allows at least the most energetic fluctuations and the whole inertial subrange to be measured. This was checked through a beforehand spectral analysis performed with a Hewlett-Packard Dynamic signal analyser model 3561A. Tests showed that the averaged “physical cut-off frequency”, derived from examination of the -2 dB attenuation point of the energy spectra, was of the order 150 Hz inside the street cavity, i.e. below the sensing cut-off frequency. Within the relevant frequency range, the whole $-\frac{5}{3}$ slope region of the spectra was fully represented for all points in the test street (see for example Fig. 7 in Section 3.2). Therefore, it was concluded that the technique was appropriate for the present investigations.

A beforehand estimation of the minimum sampling duration likely to be required in the present experimental configuration was inferred from relation (3) below derived by Lumley and Panofsky (1964) for a random variable Φ in an ergodic flow. Thus, if σ_{Φ}^2 is the variance of the prediction error committed in the estimation by $\bar{\Phi}$ of

⁴The expression “turbulence intensity of concentration fluctuations” is used in reference to the usual terminology “turbulence intensity” which, though it usually implicitly concerns velocity fluctuations, can be extended to any random variable. Its present definition, hence, copies that of the turbulence intensity of velocity fluctuations exactly (see Section 3.2).

the true mean of Φ , the sampling duration, T , must satisfy

$$T \geq 2 \frac{\overline{\phi^2} I_\phi}{\overline{\Phi}^2 \varepsilon^2} \tag{3}$$

to achieve a relative error $\sigma_\phi/\overline{\Phi}$ smaller or equal to ε . $\overline{\Phi}$ and ϕ are the time-averaged mean of Φ over the period T , and the fluctuating component of Φ , respectively, following the Reynolds statistical decomposition. I_ϕ is the integral time scale of Φ . I_ϕ is given by I/U_{adv} , where I is the integral length scale of Φ . The ratio $\overline{\phi^2}/\overline{\Phi}^2$ actually is the square of the turbulence intensity of the variable Φ . With Φ representing concentrations, we shall assume in the present case that I is of the order of the height of the buildings (6 cm), and we shall take $\overline{\phi^2}/\overline{\Phi}^2$ of the order of 40% (see Section 3.2). It yields for a free stream velocity of 3 m s^{-1} and for various values of ε ,

ε (%)	T (s)
1	1080
2	270
5	45
10	10

Specific tests showed that an averaging/sampling time of about 40 s was required to reach a mean concentration value which then does not deviate more than $\pm 5\%$ from the final time-averaged value obtained for 5 min sampling duration. One minute averaging additionally ensured an acceptable repeatability in the measurement of second-order moments.

The relationship between velocity, time and distance ($U = x/t$) entails that lengths and times are identically scaled in wind tunnel experiments since similitude requirements of physical modelling impose that velocities

in model and nature are the same. Therefore, would the same experiment be reproduced in nature under identical steady boundary conditions, sampling duration should be about 8 h to ensure a repeatability degree in measurements similar to that obtained in the wind tunnel. This is hardly achievable, and it emphasises the fact that physical modelling remains one of the most consistent and rational approaches with respect to the analysis contemplated here.

3. Experimental results

Concentration time series were recorded at 49 locations in the street cavity for z up to 60 mm, and at 21 additional points above the street for z up to 70 mm (Fig. 2). Data were sampled during 60 s at a data-acquisition rate of 400 Hz to avoid aliasing errors (the Nyquist criterion). Signals from the concentration probe were post-processed digitally to obtain the desired mean values, variances and related statistical quantities. The relevant energy spectra, probability density functions and autocorrelation functions were analysed. The corresponding results, however, are not entirely discussed in this paper.

Because the wind tunnel draws air from the room and exhausts into the same room, the background concentration of tracer steadily increases with time in the wind tunnel during experiments. However, dispersion and diffusion in the flow downwind of the test canyon and in the ambient air of the laboratory hall reduce the concentration of ethane re-entering the wind tunnel by several orders of magnitude compared with the mean concentration level in the test canyon. Thus, the background concentration typically moves from 0.34 ppm (normal ambient concentrations of hydrocarbon) to about 5 ppm after 90 min of steady release of the tracer mixture. This represents only about 1.5% of the value obtained after

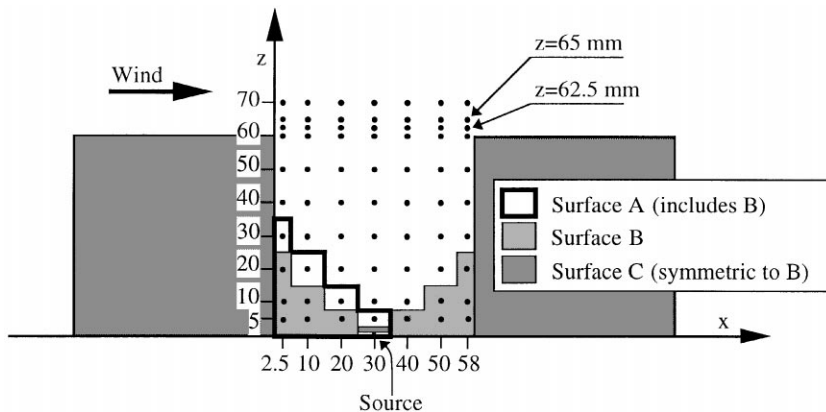


Fig. 2. Sampling locations within the test cross-section.

integration of the measured mean concentrations over the test cross-section. Therefore, the background concentration of hydrocarbon was not measured in this case⁵. Note, however, that ambient air instead of synthetic air was used to adjust the zero of the device during calibration.

3.1. Mean concentrations

For consistency with earlier results (Meroney et al., 1996), the concentration measurements are presented in terms of the ratio $K = CU_{\text{ref}}HL/Q_e$ where C is the actual measured concentration (ppm), U_{ref} the free-stream velocity (m s^{-1}) taken at 650 mm above the floor ($z_{\text{ref}} \approx 11H$) in the free-stream region of the flow above the test street, H the height of physical model of building (m), and Q_e/L the line source strength ($\text{m}^2 \text{s}^{-1}$) in which Q_e denotes ethane flow rate and L is the source length.

Fig. 3 shows the spatial distribution of \bar{K} over the test cross-section. Interpolated contours depict well the main street vortex and the wrapping of the fluid around an axis parallel to the street direction and located approximately at two thirds of the building height for $x/H \approx 0.5$. The parallel iso-concentration lines in the upper part of the canyon suggest that the approaching wind compels the main vortex, *in average*, to remain confined within the urban canopy, as was observed by Meroney et al. (1996).

Though slightly underestimated, by-eye-extrapolated values at the street walls are qualitatively in good agreement with earlier results (Fig. 4)⁶. Sufficient precautions were taken in the experiments so that the observed departure is unlikely to be attributable to a possible blockage effect from the combustion chamber, which would lead to an acceleration of the above-roof flow and, thus, entail a better ventilation of the street. Interpolation approximations related to the contouring process are also small although the software Spyglass[®] Transform used for that purpose would ideally require a larger set of input data points from a finer measurement grid. The observed discrepancies may rather be attributed to the differences inherent to the two sampling techniques used, on one hand by Meroney et al. (1996) and, on the other hand, by the authors in the present investigation. In the Meroney et al. experiments, wall concentrations were determined out of gas samples collected from flush mounted wall taps with tube inlet diameters and drawing velocities at the sampling tube inlets different from those

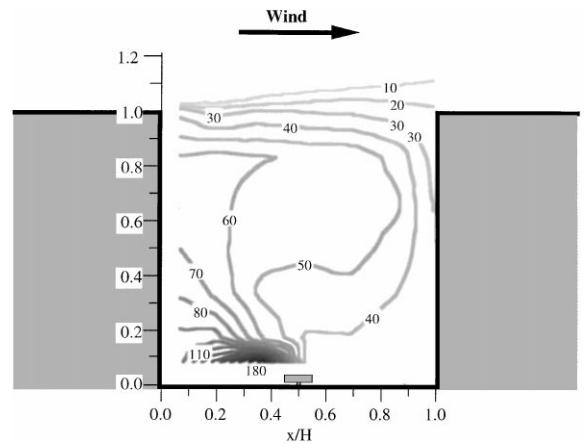


Fig. 3. Spatial distribution of mean concentration \bar{K} in the test cross-section.

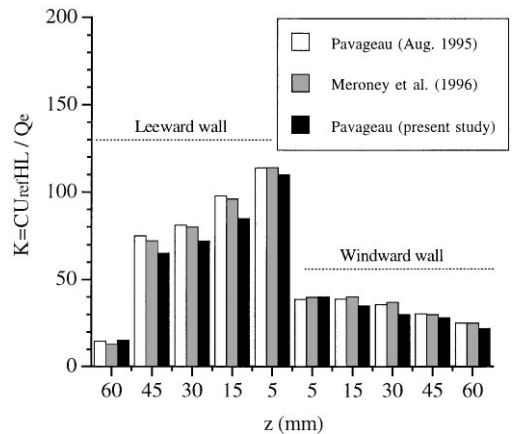


Fig. 4. Distribution of mean concentrations \bar{K} at the walls of the test street, comparison of present and earlier results.

of the sampling capillary tip of the fast FID device. Remember that exact point-measurements cannot be achieved but that measured quantities are always volume-averaged quantities over the measurement volume. The difference between the spatial resolution of measurements with the two techniques above may thus satisfactorily explain the observed discrepancies. This is all the more true for points located in regions with steep concentration gradients.

Very steep concentration gradients exist in the wake of the source and in the leeward lower corner of the test canyon. There, small differences in receptor positioning may yield large variations of measured mean concentrations because of the large values of $\partial \bar{K} / \partial x$ and $\partial \bar{K} / \partial z$. Thus, taking into account that spatial resolutions are different in field measurements, wind tunnel measurements and numerical computations, it is not surprising

⁵ This point actually raised other questions which have been discussed in more details by Pavageau (1996).

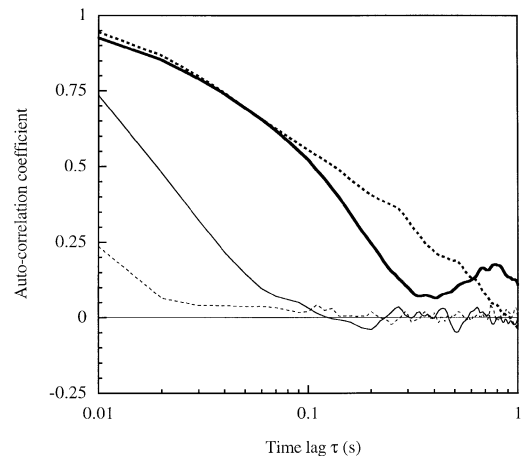
⁶ Note that the latter have furthermore been successfully compared with those of various authors (Pankus, 1995 and references therein).

that discrepancies, sometimes large, exist between the relevant experimentally or computationally estimated mean concentrations for a given case. Remember earlier comments about Fig. 4. Additionally (and in contrast to the EU directive 85203/EEC indicating that sensors have to be mounted where highest concentrations are expected), it may be recommended to avoid the positioning of concentration receptors for monitoring purposes in the leeward lower quarter of the street.

Three regions of relatively smooth concentration gradients are identified (i) at the windward lower corner, (ii) along the upper half of the leeward wall for z/H about 0.7, and (iii) around the vortex centre. The first area is a recirculation zone in which pollution is entrapped in a secondary corner vortex. The second “dead fluid” zone results from the combined action of a pressure force exerted downwards on the upper urban canopy layer by the approaching flow before it is drawn into the street canyon, and of the centrifuge inertial force undergone by the recirculating mass of fluid. In these regions, concentration signals remain auto-correlated remarkably longer than in the rest of the street (Fig. 5). For a wind direction perpendicular to the street axis, these three regions appear like suitable locations for setting up air quality monitoring stations although the last one is less convenient from a practical point of view. The examination of the level of turbulence in these regions will say whether they are definitely appropriate for air pollution monitoring.

The fast increase of spacing between the isolines downstream of the source reflects the speed with which pollution is dispersed just after its emission. There, the terms of mean advection and turbulent transport may form the dominant contribution to the balance of the transport equation of concentration. The vertical gradient $\partial\bar{K}/\partial z$ is large in the upper layer of the urban canopy while the longitudinal gradient $\partial\bar{K}/\partial x$ is nearly zero. The velocity vector is mainly oriented in the x -direction. Therefore, mean advection may not play a dominant role in pollution dispersion processes at the roof level. Oscillations of the main street vortex around its mean position yield a region at the roof interface of strong interaction between scales of turbulence inside the street and in the lower surface sublayer. Therefore, it is anticipated that turbulent mechanisms prevail over other dispersion mechanisms at the roof interface. A comprehensive analysis of the exact contribution of all physical mechanisms of dispersion would require a complete examination of the transport equation of concentration. Only simultaneous measurements of fluctuating velocities and concentrations can allow for such an analysis.

The surface integration of \bar{K} over the test cross section gives $K \approx 55$ which can be interpreted as the concentration which would be measured at any location in the street if the concentration field was fully homogeneous. It can be helpful to define \bar{K} as a pollutant retention factor,



— $z = 5 \text{ mm}; x = 20 \text{ mm}$ (source wake) — $z = 10 \text{ mm}; x = 58 \text{ mm}$ (lower windward corner)
 $z = 50 \text{ mm}; x = 2.5 \text{ mm}$ (upper half of the leeward wall) $z = 60 \text{ mm}; x = 40 \text{ mm}$ (roof level)

Fig. 5. Auto-correlation coefficient $[\overline{K'(t)K'(t + \tau)}]/\overline{K'^2}$ for various locations in the test section.

and to consider this quantity for comparing various configurations and their relevant efficiency in dispersing pollution. Though restricted here to a surface integral, this retention factor could be included as “behaviour parameter” in the description of urban climatopes as they have been defined by Theurer (1993,1996). However, this parameter alone is not sufficient to describe the efficiency or deficiency of a given arrangement. Two distinct climatopes may exhibit identical retention coefficients and at the same time be characterised by dramatically different spatial distribution of pollution. Therefore, additional information should be provided along with \bar{K} , perhaps in the form of local retention factors. For example, we give the integrals over the surfaces A, B and C as defined in Fig. 2. Note that A and both B and C represent 20 and 10% of the total cross section, respectively. Surface-averaged concentrations amount to 120, 91 and 32 ppm over A, B and C, respectively. Thus, in average the density of pollution in the leeward lower corner is approximately 2.5 as much than in the rest of the street, and between 3 and 4 times as much than in the windward lower corner.

3.2. Energy of concentration fluctuations

Fig. 6 shows the spatial distribution of $\overline{K'^2}$ defined as

$$\overline{K'^2} = \overline{C'^2}(U_{\text{ref}}HL/Q_c)^2, \tag{4}$$

where $\overline{C'^2}$ is the mean square concentration fluctuation. The maximum of $\overline{K'^2}$ occurs immediately downstream of the source because, there, a high level of intermittency

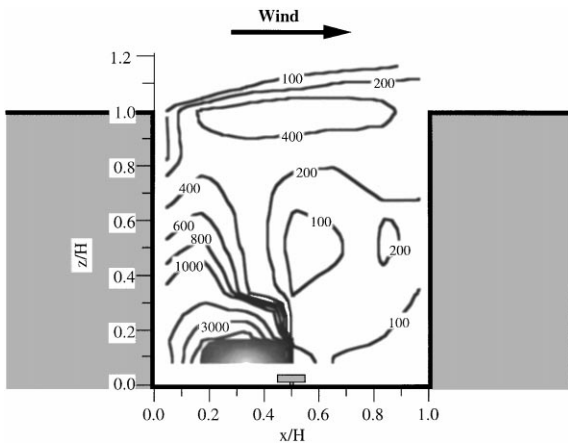


Fig. 6. Spatial distribution of the variance $\overline{K'^2}$ in the test cross-section.

exists due to both the emission of pollutant at street level suddenly mixing with the fresher air coming from the outside of the street, and the mechanical turbulence created by the periodical shedding of vortices in the wake behind the capping bar. The variance is 1 to 2 orders of magnitude lower in the rest of the canyon than in the wake of the source. It decreases downstream from the source as long as neither additional supply of pollutant nor production of turbulence exist. A secondary maximum of the concentration variance is suggested by the closed contour of Fig. 6 in the central region of the upper urban canopy. This contour can be considered as an average outline of the interaction region between the internal flow in the urban canopy and the external flow above. There, $\overline{K'^2}$ takes relatively large values because of the intermittency stemming from a flapping of the main vortex around its mean position. The corresponding spectra, one example of which is provided in Fig. 7, are characterised by a large energy containing region. The low-frequency on/off type of signals associated to the arrival of concentration pulses forms the dominant contribution to the spectra for the measurement points at the roof interface.

Time periods for which no concentration was measured, were not excluded in the calculation of the turbulence intensity of concentration fluctuations I defined as

$$I = \sqrt{\overline{K'^2}}/\bar{K}. \tag{5}$$

Turbulence intensity is the highest above the roof level ($1 \leq z/H \leq 1.17$) where it ranges from 74 to 400% disregarding the point of coordinates ($x/H = 0.04; z/H = 1$) located at the trailing edge of the upstream building where the turbulence intensity is only 27% (Fig. 8). Such high levels of turbulence are representative, again, of the

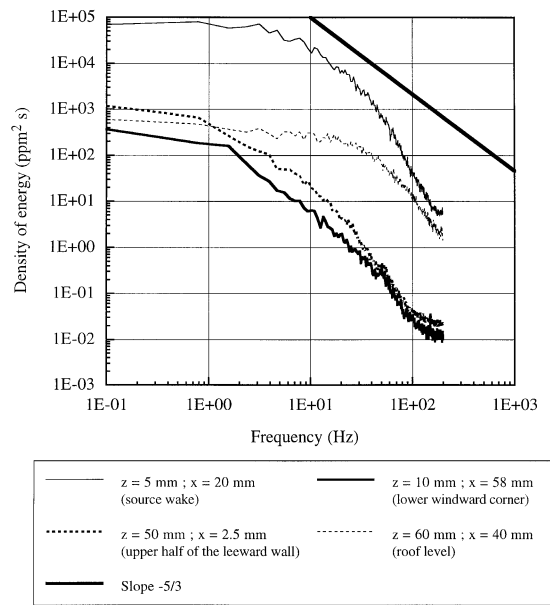


Fig. 7. Energy spectra at various locations in the tests section.

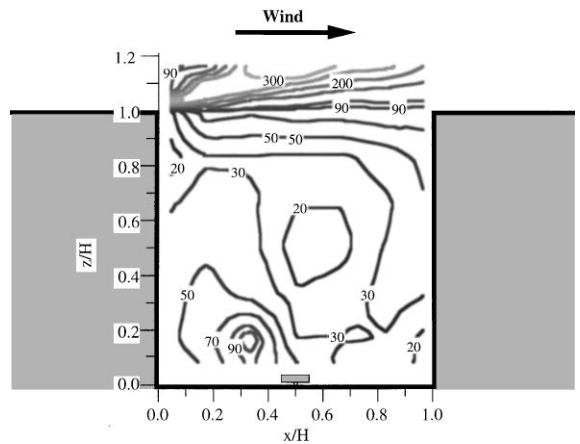


Fig. 8. Spatial distribution of the turbulence intensity of concentration fluctuations $\sqrt{\overline{K'^2}}/\bar{K}$ in the test cross-section.

intermittency of the concentration signals at the roof level.

Turbulence intensity remains rather high along the windward wall decreasing streamwise from 80% at the leading edge of the downstream building to 30% upwind of the source. No peak of turbulence was observed at mid-height where the incoming flow hits the wall. The turbulence intensity on the windward wall is not primarily of mechanical origin but mainly reflects, again, the intermittent mixing of the incoming “fresh” air with the recirculating polluted air. Turbulence intensity is about 25% just before the flow passes over the source capping

bar. Slightly above the source and immediately behind, the turbulence intensity steps up to about 110%. It remains high in the leeward corner, then decreases again with downwind distance from the source down to 30%. As was already discussed, the high level of concentration turbulence intensity close to the source stems from the intermittent dragging of pollution in the main street vortex by the wake vortices detaching behind the capping bar. The shedding of vortices behind the obstacle formed by the strip of metal above the source fosters the dispersion of the tracer gas. Would emissions be simulated in another way without the need for a capping bar like that used in this experiment, it is likely that the mean and turbulent characteristics of the concentration field in the test street would be different. According to the geometrical scaling of the model, the capping bar is a good scaled down representation of queuing vehicles. Therefore, it is suggested that the obstacle formed by vehicles and the relevant induced turbulence be accounted for in modelling, independently of whether vehicles are in motion or not.

The two entrainment regions identified in the lower windward corner and in the upper half of the leeward wall are characterised by a level of turbulence below 20%, i.e., relatively lower than in the remainder of the street. In contrast, the leeward lower corner is characterised by a relatively high level of turbulence of about 40%. These results support earlier recommendations with respect to where receptors should preferably be installed for monitoring purposes.

The energy spectra in the regions of fluid entrainment are marked by a very wide inertial subrange extending nearly over 2 decades. Two examples are given in Fig. 7. One spectrum typical of the energy distribution of concentration fluctuations in the wake of the source is additionally given for comparison. Note that spectra in the rest of the street, except for points at the roof interface, exhibit a shape similar to that for position $x = 20$ mm and $z = 5$ mm (source wake) with an overall shift towards lower energy levels.

3.3. Other statistical quantities

Minimum and maximum concentrations are subject to great variability from one experiment to another. Therefore, they are not of prime interest as long as no information concerning their frequency of occurrence is given. However, from a regulatory point of view it is of interest to be able to predict values and positions of maximum concentrations to check for exceedence of critical thresholds.

The 99-percentile, i.e., the value which is exceeded only 1% of the time, was derived from the probability density functions for all the measurement points. Fig. 9 presents the results in terms of the ratio of K_{99} to \bar{K} . This ratio is nearly constant in the street except in the wake of the source where a maximum of about 6 was observed locally. This was expected in view of the results presented

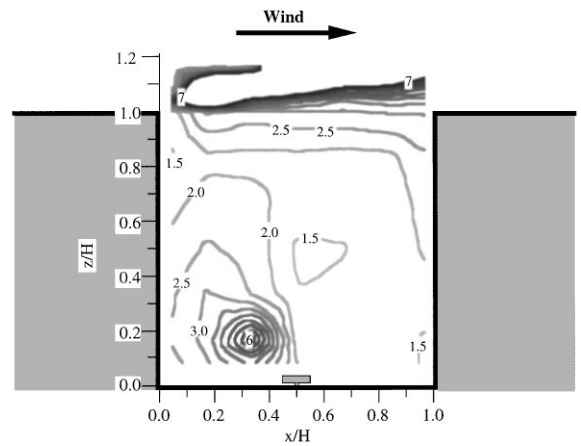


Fig. 9. Spatial distribution of the 99-percentile to mean concentration ratio in the test cross-section.

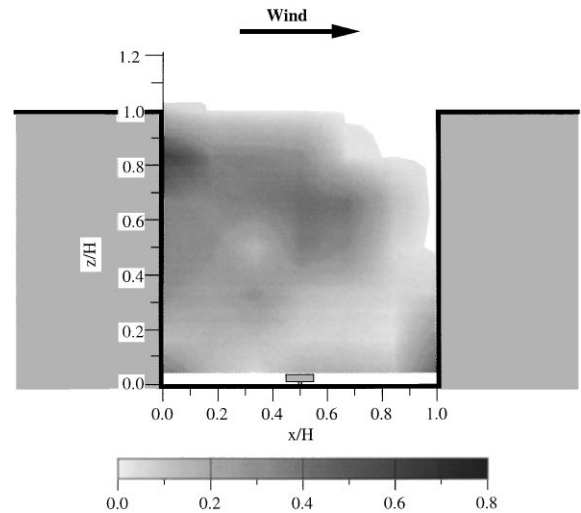


Fig. 10. Spatial distribution of the minimum-to-mean-concentration ratio in the test cross-section.

earlier. The surface-integrated value of K_{99}/\bar{K} is about 2.2. For comparison, the surface-integrated value of K_{\max}/\bar{K} was found to be about 6 in the street. However, K_{\max}/\bar{K} is of order 10 in the vicinity of the source with a maximum of 22 measured in the immediate wake of the source. In the two regions already proposed as potential candidates for the installation of monitoring devices, K_{99}/\bar{K} remains close to 1.5 in accordance with the low levels of turbulence in these regions of the street.

The examination of the spatial distribution of K_{\min}/\bar{K} is also interesting in that sense that it can provide town planners with a simple visual tool to quickly identify configurations with beneficial or adverse effects on street ventilation. Fig. 10 shows a rather large area for which

this ratio is zero or nearly zero indicating the extent of penetration of “clean” air inside the canyon. At the windward lower corner and slightly below the leeward upper corner K_{\min}/\bar{K} takes the highest values. For comparison, the 1-percentile defined as the value which is exceeded 99% of the time, is about 0.6 in these areas and in the central part of the canyon. This, together with the examination of K_{\max}/\bar{K} in the same regions confirms the presence of two areas of local trapping of fluid with weak deviations from the mean.

4. Conclusion

The case of a steady release of a tracer gas at street level in a street canyon amidst urban roughness was investigated through a wind tunnel experiment. Although it may appear redundant to focus again on this widely studied case, the difference between this analysis and earlier works lies in the full statistical description which is provided of the concentration field in the test street.

Time series of fluctuating concentrations were taken with a fast FID device at a large number of points. This was done with the view to providing model developers with a comprehensive data set corresponding to a simple test case which can be simulated numerically with little computational effort.

The paper wants to put forward an approach different from that customarily taken, and to show what can be expected from this approach, rather than to bring new insights in the field. For this reason, the paper restricts itself mainly to the presentation of results concerning mean concentrations and variances.

It has been pointed out that, for this configuration at least, placing concentration probes in the region of highest concentrations for monitoring purposes is not necessarily the best choice. With further measurements for other wind directions and building arrangements, the present approach should subsequently assist in drawing specifications for siting monitoring networks. The knowledge of the characteristic scales of turbulence developing within urban street canyons should, besides, allow the determination of appropriate values for volume and time averaging, sampling frequency and sensor location.

The interaction between the internal and external flows was clearly demonstrated in the analysis of the mean square of concentration fluctuations. Other results suggest that vehicle-induced turbulence is not only a matter of vehicle motion. Instead, the blockage effect caused simply by the presence of vehicles in the street suffices to noticeably affect the pollution distribution in the street and its dispersion. More generally, the blockage effect of any obstacle present in the canyon on concentration dispersion should perhaps deserve more attention in modelling.

For completeness of the work, the same approach should now be extended at least to other wind directions for the same geometrical configuration. For model refinement purposes, future investigations will have to include simultaneous measurements of fluctuating velocity and concentration to allow for an examination of all transport equations.

Acknowledgements

This work was made possible through financial support by the EU in the form of a Human Capital and Mobility Fellowship, and by the State of Baden-Württemberg within the framework of the PEF Project 2 96 001 (Projekt Europäische Forschung). The authors also extend sincere thanks to the following individuals for their technical competence, useful advice and constant care in assisting this work: Gopal Krishan and Thomas Glanert.

References

- Chatwin, P.C., Sullivan, P.J., 1993. The structure and magnitude of concentration fluctuations. *Boundary-Layer Meteorology* 62, 269–280.
- De Paul, F.T., Sheih, C.M., 1984. A study of pollutant dispersion in an urban street canyon. Report no. ANL/ER-84-1. Argonne National Laboratory, Argonne, IL.
- Donat, J., 1989. Bestimmung von turbulenten Größen in einer neutral geschichteten Windkanalgrenzschicht mit Hilfe einer Drei-Draht-Heißfilmsonde. Diplomarbeit Report. Meteorologisches Institut der Universität Hamburg (in German).
- Golden, J., 1961. Scale model techniques. M.S. thesis, New York University, College of Engineering, 50 pp.
- Hanna, S.R., 1993. Uncertainties in air quality model predictions. *Boundary-Layer Meteorology* 62, 3–20.
- Hoydysh, W.G., Griffiths, R.A., Ogawa, Y. 1974. A scale model study of the dispersion of pollution in street canyons. APCA paper no. 74-157, 67th Annual Meeting of the Air Pollution Control Association, Denver, CO, 9–13 June, 1974.
- Irwin, H.P.A.H., 1979. Design and use of spires for natural wind simulation. National Research Council Canada, N.A.E. Report no. LTR - LA - 233. Ottawa, Canada, August 1979.
- Irwin, H.P.A.H., 1981. The design of spires for wind simulation. *Journal of Wind Engineering and Industrial Aerodynamics* 7, 361–366.
- Kristensen, L., 1994. Recurrence of extreme concentrations. In: Gryning, S.-V., Millán, M.M. (Eds.), *Air Pollution Modelling and Its Application X*. Plenum Press, New York, 1994.
- Lumley, J.L., Panofsky, H.A., 1964. *The Structure of Atmospheric Turbulence*. Interscience, New York, pp. 36–37.
- Meroney, R.N., Pavageau, M., Rafailidis, S., Schatzmann, M., 1996. Study of line source characteristics for 2-D physical modelling of pollutant dispersion in street canyons. *Journal*

- of Wind Engineering and Industrial Aerodynamics 62, 37–56.
- Nakamura, Y., Oke, T.R., 1988. Wind, temperature and stability conditions in an east–west oriented urban canyon. *Atmospheric Environment* 22, 2691–2700.
- Oke, T.R., 1988. *Boundary Layer Climates*, second ed. Methuen, New York.
- Olesen, H.R., 1995. Toward the establishment of a common framework for model evaluation. In: Gryning, S.E., Schiermeier, F. (Eds.), *Pre-prints of the 21st NATO/CCMS International Technical Meeting on Air Pollution Modelling and Its Application: 363-70*, Plenum Press, New York, 6–10 November 1995.
- Pavageau, M., 1996. Concentration fluctuations in urban street canyons – groundwork for future studies. Technical Report. Meteorological Institute of the University of Hamburg, 97 pp. (available on request at the author's present address).
- Pankus, H., 1995. Ein mikroskaliges diagnostisches Strömungs- und Ausbreitungsmodell für komplex bebautes Gelände, Evaluierung und Validität. Diplomarbeit report im Fach Meteorologie, Hamburg University (in German).
- Plate, E., 1982. *Engineering Meteorology*, vol. 1. Fundamentals of Meteorology and their Application to Problems in Environmental and Civil Engineering. Elsevier, Amsterdam, p. 578.
- Snyder, W.H., 1972. Similarity criteria for the application of fluid models to the study of air pollution meteorology. *Boundary-Layer Meteorology* 3, 113.
- Snyder, W.H., 1992. Some observations of the influence of stratification on diffusion in building wakes. Presented at the Institute of Math and Its Application Meeting on Stably Stratified Flows. University of Surrey, Guilford, UK.
- Theurer, W., 1993. Ausbreitung Bodennaher Emissionen in komplexen Bebauungen. Ph.D. Report. IHW, University of Karlsruhe.
- Theurer, W., 1996. A classification of urban building patterns for air pollution studies. *Proceedings of the International Conference on Urban Climatology*, 10–14 June 1996, Essen, Germany, pp. 107–109.
- Wilson, D.J., 1995. Concentration Fluctuations and Averaging Time in Vapor Clouds. *American Institute of Chemical Engineers (Eds.)*, New York, ISBN 0-8169-0679-3.